Title

Heterozygous Inactivation of the Na/Ca Exchanger Increases Glucose-Induced Insulin Release, β-Cell Proliferation, and Mass

Journal

Diabetes, 60(8)

ISSN

0012-1797

Authors

Nguidjoe, Evrard
Sokolow, Sophie
Bigabwa, Serge
et al.

Publication Date

2011-08-01

DOI

10.2337/db10-0924

Peer reviewed

Heterozygous Inactivation of the Na/Ca Exchanger Increases Glucose-Induced Insulin Release, β-Cell Proliferation, and Mass

Evrard Nguidjoe,[1] Sophie Sokolow,[1,2] Serge Bigabwa,[1] Nathalie Pachera,[1] Eva D'Amico,[2] Florent Allagnat,[3] Jean-Marie Vanderwinden,[4] Abdullah Sener,[5] Mario Manto,[6] Marianne Depreter,[7] Jan Mast,[7] Geraldine Joanny,[8] Eduard Montanya,[8] Jacques Rahier,[9] Alessandra K. Cardozo,[3] Décio L. Eizirik,[3] Stéphane Schurmans,[2] and André Herchuelz[1]

OBJECTIVE—We have previously shown that overexpression of the Na-Ca exchanger (NCX1), a protein responsible for Ca^{2+} extrusion from cells, increases β-cell programmed cell death (apoptosis) and reduces β-cell proliferation. To further characterize the role of NCX1 in β-cells under in vivo conditions, we developed and characterized mice deficient for NCX1.

RESEARCH DESIGN AND METHODS—Biologic and morphologic methods (Ca^{2+} imaging, Ca^{2+} uptake, glucose metabolism, insulin release, and point counting morphometry) were used to assess β-cell function in vitro. Blood glucose and insulin levels were measured to assess glucose metabolism and insulin sensitivity in vivo. Islets were transplanted under the kidney capsule to assess their performance to revert diabetes in alloxan-diabetic mice.

RESULTS—Heterozygous inactivation of *Ncx1* in mice induced an increase in glucose-induced insulin release, with a major enhancement of its first and second phase. This was paralleled by an increase in β-cell proliferation and mass. The mutation also increased β-cell insulin content, proinsulin immunostaining, glucose-induced Ca^{2+} uptake, and β-cell resistance to hypoxia. In addition, $Ncx1^{+/-}$ islets showed a two- to four-times higher rate of diabetes cure than $Ncx1^{+/+}$ islets when transplanted into diabetic animals.

CONCLUSIONS—Downregulation of the Na/Ca exchanger leads to an increase in β-cell function, proliferation, mass, and resistance to physiologic stress, namely to various changes in β-cell function that are opposite to the major abnormalities seen in type 2 diabetes. This provides a unique model for the prevention and treatment of β-cell dysfunction in type 2 diabetes and after islet transplantation. ***Diabetes*** **60:2076–2085, 2011**

From the [1]Laboratory of Pharmacology, Université Libre de Bruxelles, Faculté de Médecine, Brussels, Belgium; the [2]Laboratory of Experimental Medicine, Université Libre de Bruxelles, Faculté de Médecine, Brussels, Belgium; the [3]Laboratory of Neurophysiology, Université Libre de Bruxelles, Faculté de Médecine, Brussels, Belgium; the [4]Laboratory of Experimental Hormonology, Université Libre de Bruxelles, Faculté de Médecine, Brussels, Belgium; the [5]Institute of Interdisciplinary Research, Institute of Molecular Biology and Medicine (IRIBHM-IBMM), Université Libre de Bruxelles, Faculté de Médecine, Brussels, Belgium; the [6]Laboratory of Experimental Neurology, Université Libre de Bruxelles, Faculté de Médecine, Brussels, Belgium; the [7]Veterinary and Agrochemical Research Centre, VAR-CODA-CERVA, Brussels, Belgium; the [8]Laboratory of Diabetes and Experimental Endocrinology, Institut d'Investigació Biomèdica de Bellvitge–University of Barcelona, Centro de Investigación Biomédica en Red de Diabetes y Enfermedades Metabolicas Asociadas (CIBERDEM), Barcelona, Spain; and the [9]Department of Pathology, Faculty of Medicine, Université Catholique de Louvain, Brussels, Belgium.

Corresponding author: André Herchuelz, herchu@ulb.ac.be.

Received 1 July 2010 and accepted 28 April 2011.

DOI: 10.2337/db10-0924

This article contains Supplementary Data online at http://diabetes.diabetesjournals.org/lookup/suppl/doi:10.2337/db10-0924/-/DC1.

E.N. and S.So. contributed equally to this work.

S.So. is currently affiliated with the University of California–Los Angeles School of Nursing, Los Angeles, California.

S.Sc. is currently affiliated with Unité de Biochimie, Département des Sciences Fonctionnelles, Faculté de Médecine Vétérinaire, Groupe Interdisciplinaire de Génoprotéomique Appliquée Research, Université de Liège, Liège, Belgium.

The prevalence of type 2 diabetes is progressing in an alarming way in most regions of the world (1,2). Type 2 diabetes is a complex disease characterized by insulin resistance and β-cell dysfunction. One of the earliest abnormalities occurring in this disease is the alteration in pulsatile insulin release with the suppression of the first phase of insulin response to glucose (3). The second phase of insulin release is also diminished and a number of abnormalities of continuous insulin release have been observed (4,5). In addition to a defect in β-cell function, a reduction in islet and β-cell mass has been observed (6,7). This reduction could be related to increased programmed cell death (apoptosis), to decreased β-cell replication, or both (8).

In a previous work, we observed that overexpression of the Na/Ca exchanger (isoform 1: Na-Ca exchanger [NCX1]), a protein responsible for Ca^{2+} extrusion from cells (9,10), increased β-cell apoptosis and reduced β-cell proliferation (11). The increase in apoptosis resulted from endoplasmic reticulum (ER) Ca^{2+} depletion with resulting ER stress (11).

If it is possible to increase apoptosis and to decrease β-cell proliferation by increasing the activity of NCX1, it may be possible to obtain the opposite effects by downregulating such a mechanism. To test this hypothesis, we generated *Ncx1* heterozygous deficient mice ($Ncx1^{+/-}$). Our data show that $Ncx1^{+/-}$ heterozygous inactivation induces several β-cell modifications, including an increase in glucose-induced insulin release and in β-cell proliferation and mass. $Ncx1^{+/-}$ islets also displayed an increased resistance to hypoxia, and when transplanted in diabetic animals, showed a two- to four-times higher rate of diabetes cure than $Ncx1^{+/+}$ islets.

RESEARCH DESIGN AND METHODS

Generation of $Ncx1^{-/-}$ mice. Exon 11 of the murine *Ncx1* gene (GenBank, accession number AF409089) was cloned from a 129/Sv genomic phage library. The first 206-bp were amplified by PCR and a *Bam*HI site was introduced for cloning. A targeting vector was constructed by inserting the

neomycin resistance cassette (neo) into the *Bam*HI restriction site of that amplified exon. Standard procedures were used to generate $Ncx1^{+/-}$ mice (12). Except as otherwise stated, experimental mice were 2 to 6 months old, of both sexes, and had F2 genetic backgrounds from 129/Sv and CD1 mice. $Ncx1^{+/+}$ mice consisted of age-matched littermates with two wild-type (WT) alleles at the *Ncx1* locus ($Ncx1^{+/+}$).

Intracellular Ca^{2+} concentration measurements. The measurement of intracellular Ca^{2+} concentration using fura-2 was done, as previously described (11,13), using a camera-based image analysis system (MetaFluor, Universal Imaging, Ypsilanti, MI).

Time-frequency analysis of spectral densities of the Ca^{2+} oscillations was computed using Ackqnowledge Software, (Biopac Systems, Goleta, CA), with a Hamming window. Data were segmented in successive epochs of 1 min. We computed the power spectral density (PSD), the integral below the power spectrum for the frequency band 0–0.17 Hz, and the crest factor for the same frequency band (ratio amplitude of the power spectra/integral 0–0.17 Hz).

^{45}Ca uptake, insulin content, and insulin release from isolated islets. The methods used to measure ^{45}Ca uptake in intact islets and insulin release from perifused islets are described in detail elsewhere (11,13–15). Insulin was assayed using an ELISA kit (Mercodia, Uppsala, Sweden). For the measurement of insulin content, the islets were homogenized in water in the absence of glucose.

Measurement of glucose metabolism and morphology. The methods used to measure D-[5-^{3}H]glucose metabolism and D-[U-^{14}C]glucose oxidation in intact islets, have been previously described (16,17).

Golgi proinsulin/β-cell area was evaluated on slides stained for proinsulin with immunoperoxidase (18) digitized through a JVC KY-F58 color digital camera (Japan Victor, Brussels, Belgium). Tissues sections (5-μm thick) were prepared according to Jacoby et al. (19) and processed for hematoxylin-eosin staining.

For electron microscopy, groups of 30 islets were fixed, epoxide-embedded, and analyzed as described previously (20).

Measurement of β-cell proliferation, apoptosis, mass, and size. To measure β-cell proliferation, mice were injected intraperitoneally with 5-bromo-2-deoxyuridine (BrdU, Sigma-Aldrich, St. Louis, MO; 100 mg/kg body wt) 6 h before euthanasia, as previously described (21). An alternative method to measure β-cell replication was the Ki67 labeling method (rabbit monoclonal anti-Ki67, Vector Laboratories, Brussels, Belgium) with a method similar to the BrdU immunofluorescence labeling (22).

To measure β-cell apoptosis, the terminal deoxynucleotidyltransferase mediated dUTP nick-end labeling (TUNEL) method was used, with the In Situ Cell Death Detection Kit (Roche Diagnostics, Vilvoorde, Belgium). The method for β-cell labeling and counting was similar to that for β-cell proliferation.

Cell viability in vitro was measured using Hoechst 33342 (Ho342) and propidium iodide (PI) (23). The percent viability in $Ncx1^{+/+}$ single β-cells and islets (not exposed to thapsigargin or cyclopiazonic acid) was 65% to 70% and 85% to 95%, respectively. In some experiments, cytokines were used at the following concentrations: human IL-1β: 50 units/mL (R&D Systems, Oxon, UK); mouse interferon-γ: 1000 units/mL (tebu-bio, Boechout, Belgium).

Quantification of β-cell mass was performed by point-counting morphometry of insulin-peroxidase immunostained pancreatic sections, as previously described (24). Individual β-cell size was measured using the calibrated ImageJ (National Institutes of Health, Bethesda, MD) image analysis program. The β-cell area of the pancreatic section was divided by the number of β-cell nuclei identified in the area.

In vitro hypoxia studies. In vitro hypoxia studies were as previously described (25). The duration of hypoxia was 6 h. Viability of β cells was measured as described above.

Glucose metabolism, insulin sensitivity, serum glucagon, growth hormone, and glucagon-like peptide 1 measurement in vivo. The measurement of glucose metabolism and insulin sensitivity in vivo were done as previously described (26,27). Serum glucagon, growth hormone, and glucagon-like peptide 1 (GLP-1) were measured using Glucagon Human/Mouse/Rat ELISA (Alpco, Salem, NH), Rat/Mouse Growth Hormone ELISA Kit (Millipore, St. Charles, MO), and Mouse GLP-1 ELISA kit (Antibodies-online.com, Aachen, Germany).

Diabetes induction and islets transplantation. Diabetes was induced in 10- to 12-week-old C57BL6N mice using a single intravenous injection of alloxan (90 mg/kg; Sigma) (25,26). Grafts of 50 to 400 islets from $Ncx1^{+/+}$ or $Ncx1^{+/-}$ mice were transplanted under the kidney capsule in diabetic mice. Thereafter, the nonfasting blood glucose levels were measured in each animal up to 100 days, using a Glucometer (Abbott, Diegem, Belgium). Islet grafts were considered functional when the nonfasting blood glucose returned to normoglycemic levels (<220 mg/dL). In some animals, the graft-bearing kidney was removed to confirm islet graft function.

Statistics. The results are expressed as means ± SEM. The statistical significance of differences between data was assessed by using ANOVA, followed by the Tukey post-test.

RESULTS

Generation of $Ncx1^{-/-}$ mice. A mutant allele was constructed as described in RESEARCH DESIGN AND METHODS (Fig. 1*A*). After electroporation with the targeting vector, the recombinant embryonic stem cell clones were identified by DNA hybridization and used to produce chimeric mice (Fig. 1*B*). Transmission of the mutant allele produced *Ncx1* heterozygous mice that were mated to generate *Ncx1* null mutants ($Ncx1^{-/-}$). The $Ncx1^{-/-}$ mice were not viable and died during embryogenesis as described (28). Heterozygous and WT mice genotyping from tail biopsy specimen DNA revealed an *Ncx1* WT amplicon of ~250 bp and an *Ncx1* recombinant allele of ~100 bp, which were simultaneously amplified by PCR (Fig. 1*C*). NCX1 mRNA levels in batches of islets from $Ncx1^{+/+}$ and $Ncx1^{+/-}$ mice, measured using RT-PCR, showed a clear decrease in $Ncx1^{+/-}$ mice (Fig. 1*D*). $Ncx1^{+/-}$ mice were viable, fertile, had a normal body weight, and showed no macro- or microscopic abnormalities at the level of the brain, heart, lung, liver, spleen, stomach, intestine, and thymus (Supplementary Fig. 1). Likewise, serum levels of glucagon, growth hormone (GH) in the fasting state and GLP-1 in the fed state were comparable in $Ncx1^{+/+}$ and $Ncx1^{+/-}$ mice at 12 weeks (0.48 ± 0.04 vs. 0.41 ± 0.14 ng/mL, 2.4 ± 0.44 vs. 1.67 ± 0.44 ng/mL, and 3.20 ± 0.28 vs. 2.86 ± 0.15 pg/ml, respectively; $n = 4$ in each case, except for GH where n = 9–11, respectively, $P > 0.05$).

Na/Ca exchange activity in $Ncx1^{+/-}$ islets. To evaluate the functional consequences of *Ncx1* heterozygous inactivation, the activity of the Na/Ca exchanger was evaluated by measuring the effect of extracellular Na^+ removal on ^{45}Ca uptake and cytosolic free Ca^{2+} concentration ($[Ca^{2+}]_i$), and of K^+-induced membrane depolarization on $[Ca^{2+}]_i$. Removal of extracellular Na^+ increased ^{45}Ca uptake in $Ncx1^{+/+}$ and $Ncx1^{+/-}$ islets (Fig. 1*E*), the uptake in $Ncx1^{+/-}$ islets recorded in the absence of extracellular Na^+ being half of that measured in $Ncx1^{+/+}$ islets. Removal of extracellular Na^+ induced a sustained increase in $[Ca^{2+}]_i$ (Fig. 1*F*), that again was reduced in $Ncx1^{+/-}$ compared with $Ncx1^{+/+}$ islets. Thus, the increase in $[Ca^{2+}]_i$ induced by the absence of extracellular Na^+, measured as the area under the curve over the baseline value during a 5- to 25-min period was reduced by 24% in $Ncx1^{+/-}$ compared with $Ncx1^{+/+}$ islets ($P < 0.05$). K^+ increased $[Ca^{2+}]_i$ in both types of islets (Fig. 1*G*), but $[Ca^{2+}]_i$ was always slightly higher in $Ncx1^{+/-}$ than in $Ncx1^{+/+}$ mice. The difference in mean concentration was higher (36%) during the period of K^+ exposure (min 2–12) and of K^+ removal (65%; min 12–24) than during the baseline period (min 0–2; $P < 0.001$), indicating that Ca^{2+} extrusion was mainly impaired during the period of K^+ stimulation and recovery. Taken as a whole, these data indicate that partial *Ncx1* heterozygous inactivation reduces Na/Ca exchange activity in islet cells both in its forward and reverse mode. We then examined the effect of *Ncx1* heterozygous inactivation on islet function.

Islet function in $Ncx1^{+/-}$ islets

Insulin release. Figure 2*A* and *B* shows the effect of an increase in glucose concentration from 2.8 to 11.1 mmol/L on insulin release from perifused islets (*A*: representative experiment, *B*: mean of 4–6 experiments). In $Ncx1^{+/+}$ islets, glucose induced an oscillatory increase

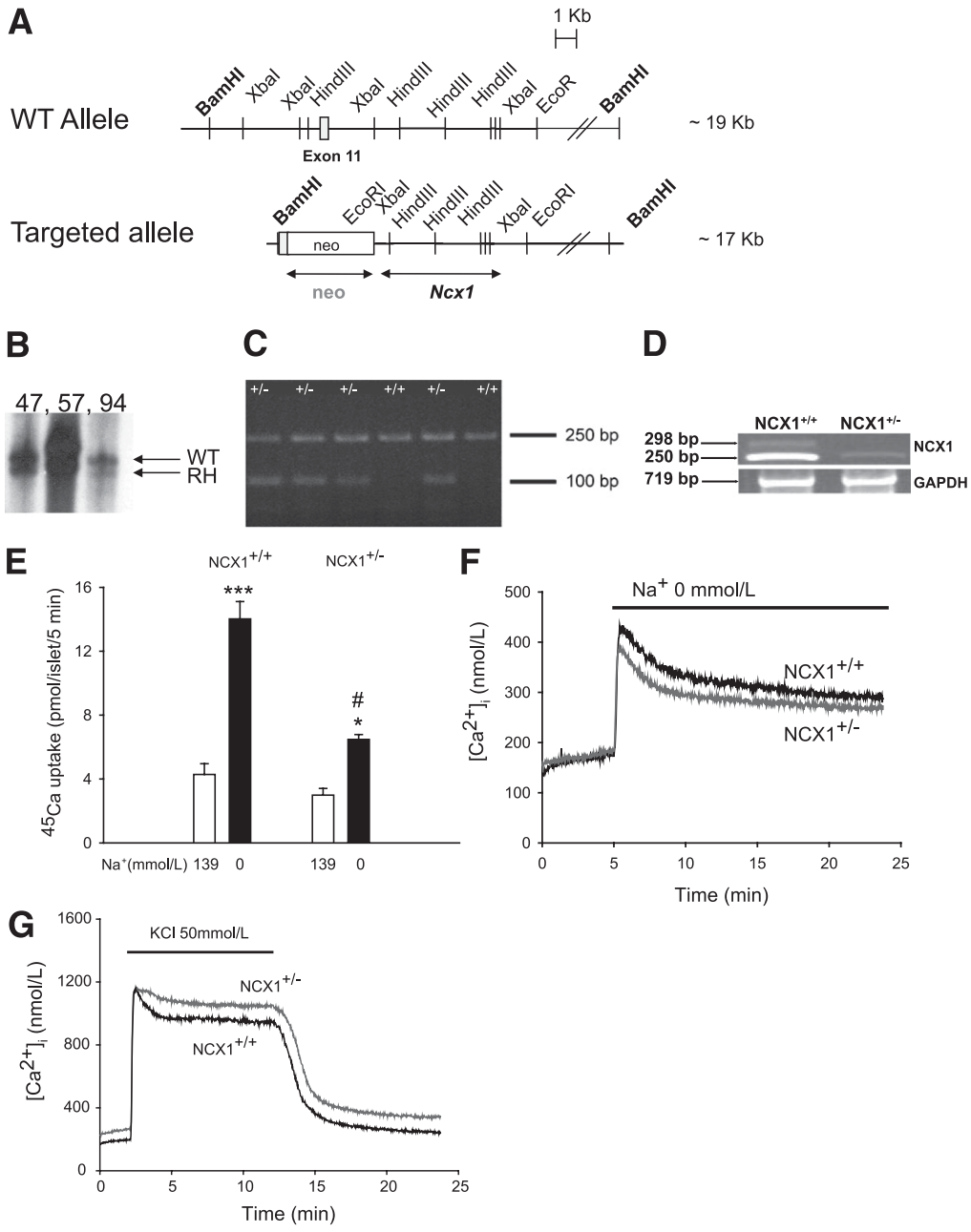

FIG. 1. Targeted disruption of the *Ncx1* gene and Na/Ca exchange activity in *Ncx1*$^{+/+}$ and *Ncx1*$^{+/-}$ islets. *A*: Structure of the WT and the targeted alleles. The eleventh exon, the neomycin resistance cassette, and the probes used in DNA and RNA hybridization analysis (bars underneath the targeted allele) are represented. *B*: DNA hybridization analysis of *Bam*HI digested genomic DNA isolated from embryonic stem cell clones using the depicted probe. RH, recombinant homolog. *C*: PCR analysis for genotyping. *D*: *Ncx1* mRNA levels in batches of islets from *Ncx1*$^{+/+}$ and *Ncx1*$^{+/-}$ mice. GAPDH, glyceraldehyde-3-phosphate dehydrogenase. *E*: ^{45}Ca uptake in the presence and the absence of extracellular Na^+. Means ± SEM of four experiments, comprising four to five replicates each. *$P < 0.05$, ***$P < 0.001$ vs. Na^+ 139 mmol/L, #$P < 0.001$ vs. *Ncx1*$^{+/+}$. *F*: Effect of extracellular Na^+ removal on $[Ca^{2+}]_i$ in *Ncx1*$^{+/+}$ and *Ncx1*$^{+/-}$ islets. The period of exposure to Na^+-free medium is indicated by a bar above the curves. The curves shown are the mean of seven traces in each case. *G*: Effect of KCl (50 mmol/L) on $[Ca^{2+}]_i$ in *Ncx1*$^{+/+}$ and *Ncx1*$^{+/-}$ islets. The period of exposure to KCl is indicated by a bar above the curves. The curves shown are the mean of 13 traces in each case.

in insulin release. In *Ncx1*$^{+/-}$ islets, glucose induced a marked first-phase insulin release, followed by a progressive increase with less clear oscillations. The amount of insulin released during the entire period of stimulation (16–60 min) was about 2.4-times higher in *Ncx1*$^{+/-}$ than in *Ncx1*$^{+/+}$ islets ($P < 0.02$). A similar observation was made at 16.7 mmol/L glucose, where the fold-increase was 1.7 ($P < 0.05$), or by perifusing a single islet, where the fold-increase in response to 11.1 mmol/L glucose was 2.6 ($P < 0.05$, Supplementary Figs. 2 and 3, respectively).

Glucose-induced increase in $[Ca^{2+}]_i$. Oscillatory insulin release is associated with oscillatory $[Ca^{2+}]_i$ increases (29,30). Figure 2*C* and *D* shows the effect of 11.1 mmol/L glucose on $[Ca^{2+}]_i$ oscillations in intact islets. *Ncx1*$^{+/+}$ islets showed a rapid increase in $[Ca^{2+}]_i$ with an initial phase, followed by a second phase displaying regular oscillations. *Ncx1*$^{+/-}$ islets also showed a rapid increase in $[Ca^{2+}]_i$ but the initial phase was more distinct, separated from the second phase, which displayed disrupted $[Ca^{2+}]_i$ oscillations. Figure 2*E* and *F* shows at a larger scale the oscillations

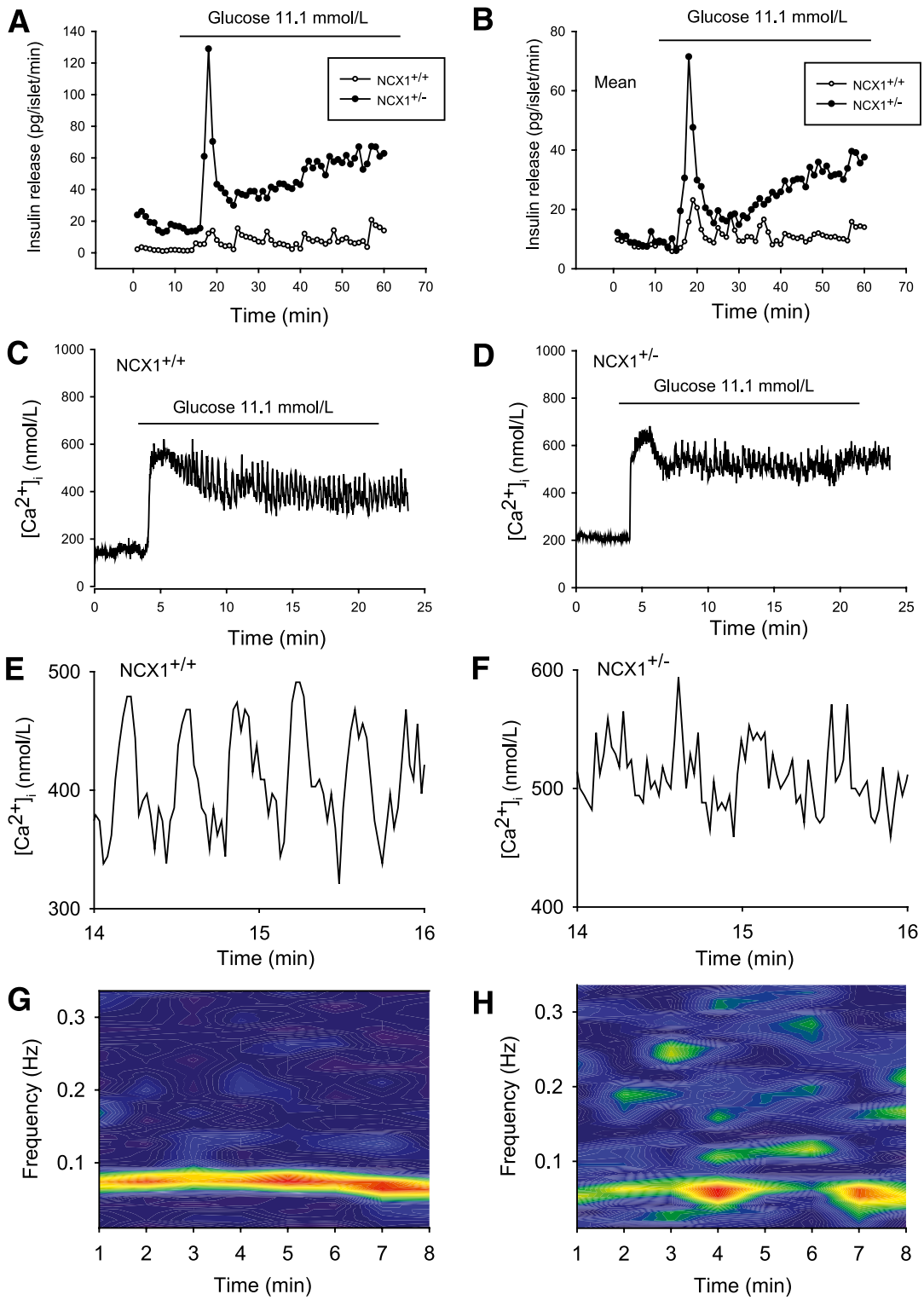

FIG. 2. Effect of *Ncx1* heterozygous inactivation on glucose-induced insulin release and $[Ca^{2+}]_i$ oscillations. Effect of 11.1 mmol/L glucose on insulin release (*A* and *B*) and $[Ca^{2+}]_i$ (*C* and *D*) from groups of 20 islets: representative experiment (*A*), mean of four ($Ncx1^{+/+}$) and six ($Ncx1^{+/-}$) individual experiments (*B*). *C* and *D* show typical individual traces observed in $Ncx1^{+/+}$ and $Ncx1^{+/-}$ islets, respectively. The curves are representative of seven and eight individual traces, respectively. The period of exposure to glucose 11.1 mmol/L is indicated by a bar above the curves. In both cases, the islets were from different mice. *E* and *F* present the same traces as in panels *C* and *D*, showing the $[Ca^{2+}]_i$ oscillations between min 14 and 16 on a larger scale. *G* and *H*: Power spectral analysis of the oscillations observed in typical individual traces. (A high-quality digital representation of this figure is available in the online issue.)

during the period 14–16 min. The number of oscillations is easily determined and counted in $Ncx1^{+/+}$ islets, at variance with $Ncx1^{+/-}$ islets, where the oscillations are irregular and difficult to identify. PSD analysis of the oscillations showed that $Ncx1^{+/+}$ islets displayed a single peak with a very stable generator in frequency and magnitude (Fig. 2*G*), whereas $Ncx1^{+/-}$ islets displayed an unstable dominant frequency and numerous peak intrusions above the frequency of 0.10 Hz,

illustrating the irregularity of the oscillations (Fig. 2*H*). Supplementary Fig. 4*A* and *B* also shows that there was a significant difference both in the magnitude of the peak of power spectra (Max PSD) and in the crest factor (ratio Max/Integral) between *Ncx1*$^{+/+}$ and *Ncx1*$^{+/-}$ islets.

Glucose metabolism. To stimulate insulin release, glucose must be metabolized by the pancreatic β-cell (31). In *Ncx1*$^{+/+}$ and *Ncx1*$^{+/-}$ islets, the utilization of D-[5-^{3}H] glucose increased as a result of the rise in the glucose concentration from 2.8 to 16.7 mmol/L (Fig. 3*A*). At the low hexose concentration, $^{3}H_2O$ generation from D-[5-^{3}H]glucose was slightly higher in *Ncx1*$^{+/-}$ than in *Ncx1*$^{+/+}$ cells.

Generation of $^{14}CO_2$ from D-[U-^{14}C]glucose was also increased in response to the rise in glucose concentration in both type of islets (Fig. 3*B*). However, although oxidation tended to be higher in *Ncx1*$^{+/-}$ islets at the low glucose concentration, glucose oxidation was significantly lower in *Ncx1*$^{+/-}$ than in *Ncx1*$^{+/+}$ cells at the high glucose concentration. As a result of these differences, the paired ratio between D-[U-^{14}C]glucose oxidation and D-[5-^{3}H]glucose utilization increased with the rise in glucose concentration in *Ncx1*$^{+/+}$ cells ($P < 0.05$), but it did not change in *Ncx1*$^{+/-}$ cells. Compared with *Ncx1*$^{+/+}$ cells, ATP generation tended to be increased in *Ncx1*$^{+/-}$ islets at low (53%) but reduced at high glucose concentration (−20%, $P < 0.05$, Supplementary Table 1).

Uptake of ^{45}Ca in response to glucose. Glucose-induced insulin release is preceded by Ca^{2+} uptake in the β-cell (32). In *Ncx1*$^{+/+}$ and *Ncx1*$^{+/-}$ islets, 16.7 mmol/L glucose stimulated ^{45}Ca uptake (Fig. 3*C*). Whereas at low glucose, there was no significant difference in ^{45}Ca uptake between the two types of islet; the increase in uptake induced by 16.7 mmol/L glucose was twice as high in *Ncx1*$^{+/-}$ than in *Ncx1*$^{+/+}$ islets.

Insulin content. In view of the major increase in insulin release in *Ncx1*$^{+/-}$ islets, the insulin content of the islets was measured and was about double that of *Ncx1*$^{+/+}$ islets (Fig. 3*D*).

Morphology. There were no differences in islet morphology or in the position of β-, α-, and δ-cells between *Ncx1*$^{+/+}$ and *Ncx1*$^{+/-}$ islets (data not shown). Proinsulin staining, however, was increased in *Ncx1*$^{+/-}$ compared with *Ncx1*$^{+/+}$ islets (Fig. 4*A*) of adult mice (12–14 weeks), a finding in line with the increase in insulin content. Electron microscopic analysis revealed no difference in the features of pancreatic β-cells, including secretory granules, nucleus, mitochondria,

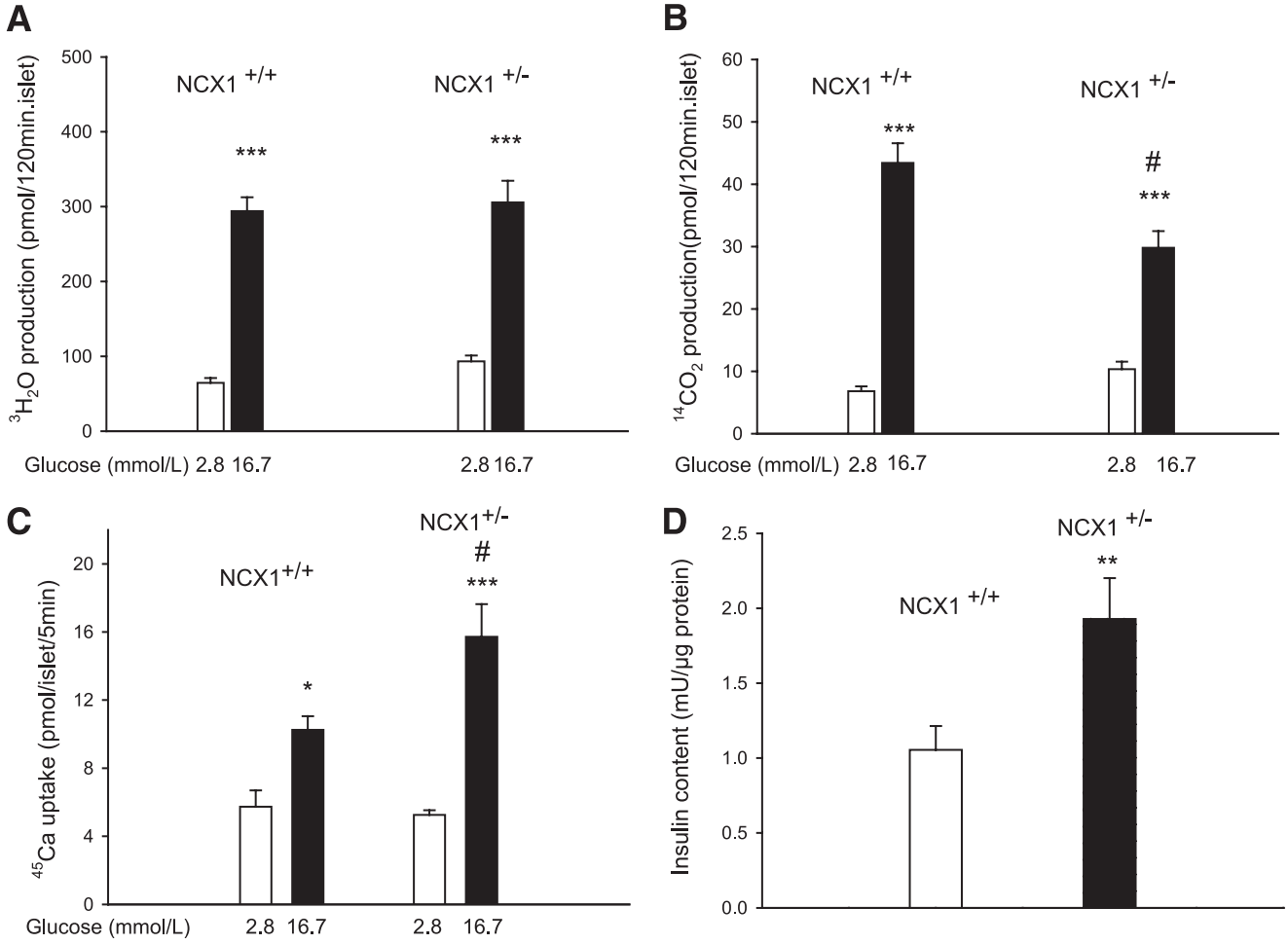

FIG. 3. Effect of *Ncx1* heterozygous inactivation on glucose metabolism, ^{45}Ca uptake, and insulin content. Metabolism of D-[5H]glucose (*A*) and D-[U-^{14}C]glucose (*B*) is shown in *Ncx1*$^{+/+}$ and *Ncx1*$^{+/-}$ islets. Mean ± SEM values are shown for 12 to 25 individual determinations. *A*: ***$P < 0.001$ vs. 2.8 mmol/L. *B*: ***$P < 0.01$ vs. 2.8 mmol/L; #$P < 0.01$ vs. *Ncx1*$^{+/+}$ islets at 16.7 mmol/L glucose. *C*: Effect of glucose on ^{45}Ca uptake in *Ncx1*$^{+/+}$ and *Ncx1*$^{+/-}$ islets. Mean ± SEM values are shown for four experiments, comprising four to six replicates in each case. *$P < 0.05$; ***$P < 0.001$ vs. 2.8 mmol/L; #$P < 0.01$ vs. *Ncx1*$^{+/+}$ islets at 16.7 mmol/L glucose. *D*: Insulin content of batches of 10 islets (means ± SEM of 14 and 7 individual determinations). **$P < 0.01$ vs. *Ncx1*$^{+/+}$ islets.

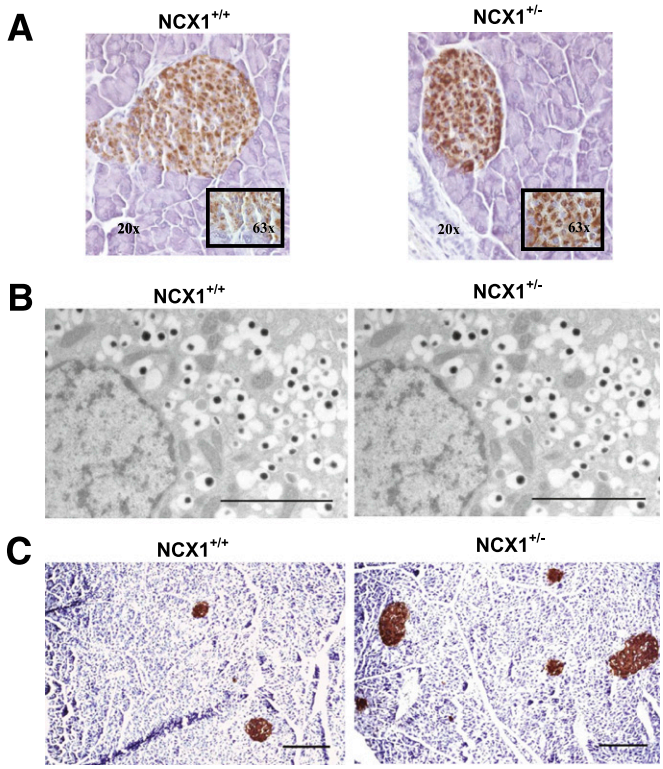

FIG. 4. Effect of *Ncx1* heterozygous inactivation on islet morphology. *A*: Immunohistochemistry: proinsulin labeling (immunoperoxidase in brown) is stronger in $Ncx1^{+/-}$ than in $Ncx1^{+/+}$ islets. Representative images of six 12-week-old mice pancreas sections in each case. *Inset*: Same image at higher magnification (original magnification ×63). *B*: Transmission electron microscopy. Groups of 30 islets from $Ncx1^{+/+}$ and $Ncx1^{+/-}$ mice were fixed, and three sections in each block demonstrating an islet were cut at randomly chosen depths. The characteristic ultrastructural features of pancreatic β-cells were comparable in both types of islets. Representative images are shown of β-cells from 12-week-old mice $Ncx1^{+/+}$ (*left panel*) and $Ncx1^{+/-}$ islets (*right panel*). Scale bar = 2 μm. *C*: Representative images of pancreatic β-cells immunolabeled with immunoperoxidase (brown) using a polyclonal anti-insulin antibody, with hematoxylin used for the counterstain. The sections were used to evaluate the β-cell mass by counting morphometry. The photomicrographs represent 12-week-old mice pancreatic sections of $Ncx1^{+/+}$ (*left panel*) and $Ncx1^{+/-}$ islets (*right panel*). Scale bar = 0.2 μm. (A high-quality digital representation of this figure is available in the online issue.)

ER, and Golgi apparatus of $Ncx1^{+/+}$ and $Ncx1^{+/-}$ adult mice (Fig. 4*B*). Quantitative analysis of relative volume of organelles demonstrated no significant difference between $Ncx1^{+/+}$ and $Ncx1^{+/-}$ β-cells (data not shown).

Taken as a whole, the data so far presented show that *Ncx1* heterozygous inactivation strongly increases glucose-induced insulin production and release.

β-Cell mass, size, proliferation, and viability. β-Cell mass, size, and proliferation was measured in young (4 weeks) and adult (12 weeks) mice (Fig. 5*A*–*C*). As expected, β-cell mass was increased at 12 weeks in both types of islet, although the increase was of much larger magnitude in $Ncx1^{+/-}$ than in $Ncx1^{++}$ islets (8.8- vs. 1.6-fold increase, respectively, $P < 0.001$; Fig. 4*C*). This increase was not due to β-cell or islet hypertrophy because no change in β-cell and islet size was observed between $Ncx1^{+/+}$ and $Ncx1^{+/-}$ mice (Fig. 5*B* and data not shown); rather, it was due to an increase in the β-cell proliferation rate. As expected, β-cell proliferation, as measured using BrdU, was decreased at 12 weeks compared with 4 weeks (Fig. 5*C*), although the decrease was of a lower magnitude in $Ncx1^{+/-}$ than in $Ncx1^{+/+}$ islets (−40 vs. −85%, $P < 0.01$). As a result, a 5.25-times higher proliferation rate was observed at 12 weeks in $Ncx1^{+/-}$ compared with $Ncx1^{+/+}$ mice (Fig. 5*C* and Supplementary Fig. 5). We also observed an increase in proliferation rate of the exocrine pancreatic cells that was lower than in the endocrine pancreas (1.7- vs. 5.25-fold increase, respectively; $P < 0.02$, Supplementary Fig. 5). Ki67 staining showed an increased labeling in $Ncx1^{+/-}$ compared with $Ncx1^{+/+}$ islets, with the number of positive nuclei averaging 2.75 ± 0.31 vs. 1.58 ± 0.28 per islet, respectively ($P < 0.01$).

Apoptosis of β-cells was also measured, but no difference could be found between $Ncx1^{+/-}$ and $Ncx1^{+/+}$ islets. Thus, whether using the TUNEL method at 4 and 12 weeks under basal conditions (Fig. 5*D*), or Ho342 and PI staining of islet cells (Fig. 5*E*–*G*) under basal or stimulated conditions created by the absence or presence of sarcoendoplasmic reticulum Ca^{2+} ATPase (SERCA) inhibitors (Fig. 5*E*), and 72-h exposure of intact islets to cytokines (Fig. 5*F*) or thapsigargin (Fig. 5*G*), no difference could be found between both types of islets.

Hypoxia studies. To test their resistance to physiologic stress, the islets were then subjected to hypoxia for 6 h, cell death being measured using Ho342 and PI staining of intact islets. Figure 5*H* shows that 71% of $Ncx1^{+/+}$ islets showed a decrease in viability <60% compared with 45% of $Ncx1^{+/-}$ islets.

Transplantation. We then transplanted $Ncx1^{+/-}$ islets under the kidney capsule of alloxan-diabetic mice to examine their performances compared with $Ncx1^{+/+}$ islets. First, we had to determine the minimum number of $Ncx1^{+/+}$ islets to transplant to cure diabetes, which must be ~300 islets. Indeed, all transplantations with 400 islets were successful, with nephrectomy leading to a reincrease in glycemia (Supplementary Fig. 6*A*), whereas the rate of success of transplantation of 200 $Ncx1^{+/+}$ islets was only 2/5 (Supplementary Fig. 6*B*). In comparison, the rate of success of transplantation of 100 $Ncx1^{+/-}$ islets was 4/5 (Supplementary Fig. 6*C*), whereas the rate of success of transplantation of 50 $Ncx1^{+/-}$ islets was 2/3 (Supplementary Fig. 5*D*). This suggests that the $Ncx1^{+/-}$ islets are at least four- to seven-times more efficient to cure diabetes than the $Ncx1^{+/+}$ islets. Finally, we performed a last series of parallel transplantations of 100 islets (Fig. 6*A* and *B*). The success rate was 4/5 and 2/5 for $Ncx1^{+/-}$ and $Ncx1^{+/+}$ islets, indicating that the $Ncx1^{+/-}$ islets are at least twice as efficient in curing diabetes than $Ncx1^{+/+}$ islets.

Morphometric analysis of the islet grafts after nephrectomy of mice who received a transplant of 100 islets showed that the relative volume of islet grafts was about seven-times higher in cured than in noncured animals (4.26 ± 1.09% vs. 0.61 ± 0.39%, respectively [n = 4–6]; $P < 0.05$), confirming that diabetes cure is attributable to islet transplantation.

Glucose metabolism and insulin sensitivity in vivo. Despite the major increase in insulin release seen in vitro, plasma glucose and insulin levels were comparable in $Ncx1^{+/-}$ and $Ncx1^{+/+}$ mice, both in the fasted and the fed state (Fig. 6*C* and *E*). However, the glucose-tolerance test showed an increased and earlier initial peak of insulin release (Fig. 6*D* and *F*), with a subsequent faster decrease in glucose levels during the ensuing 45 min (−152 ± 20 compared with −81 ± 2 mg/dL in $Ncx1^{+/-}$ and $Ncx1^{++}$ mice, respectively, $P < 0.01$). The intraperitoneal insulin sensitivity test showed no difference between the mice (Supplementary Fig. 7).

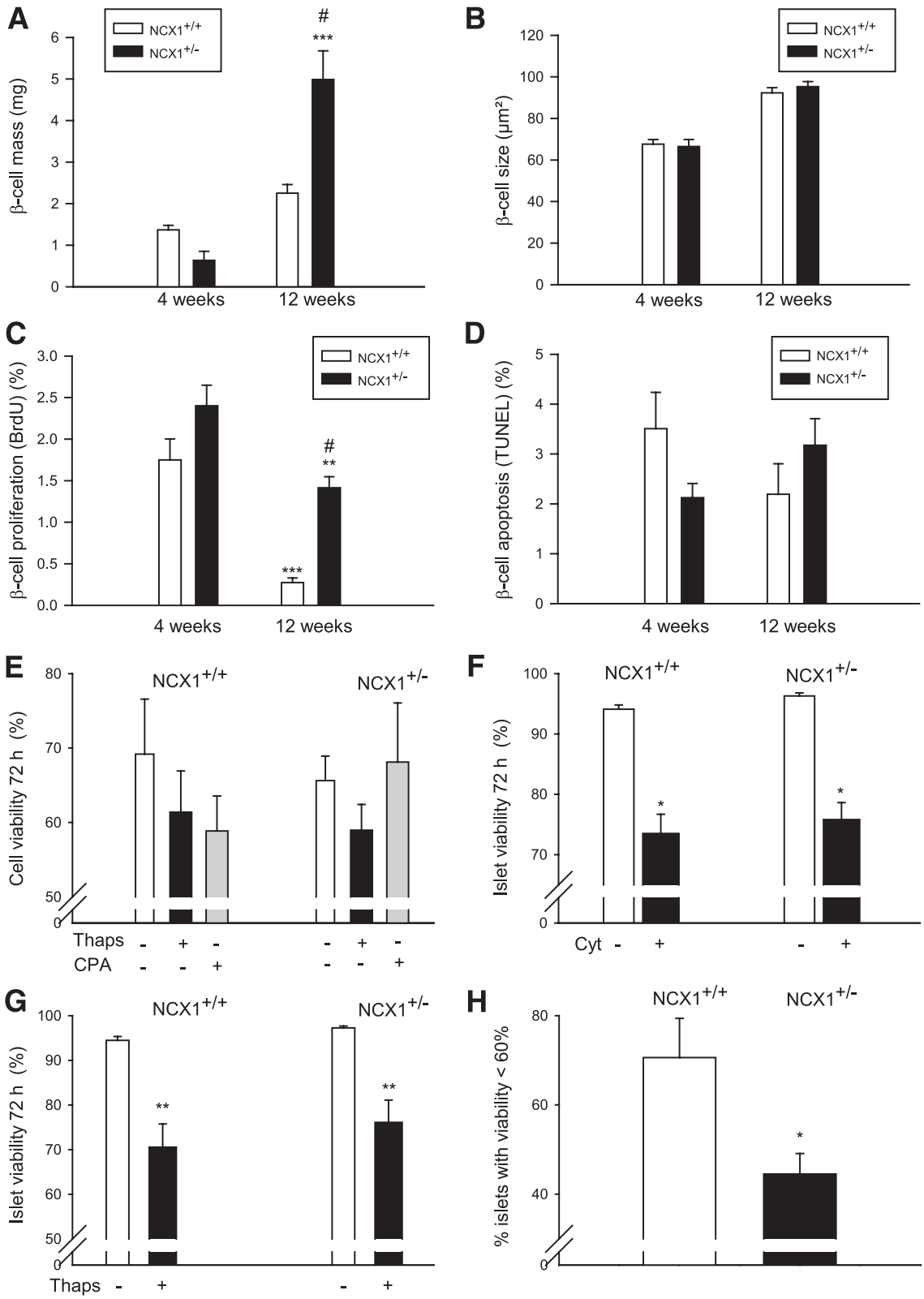

FIG. 5. Effect of *Ncx1* heterozygous inactivation is shown on β-cell mass (*A*), size (*B*), proliferation rate (*C*), and apoptosis (*D*) between weeks 4 and 12 in *Ncx1*$^{+/+}$ and *Ncx1*$^{+/-}$ mice. Mean ± SEM values are shown from five and six pancreas specimens, respectively. *A:* ***$P < 0.001$ vs. values at 4 weeks; #$P < 0.001$ vs. *Ncx1*$^{+/+}$ β-cells at 12 weeks. *C*: **$P < 0.01$; ***$P < 0.001$ vs. respective value at 4 weeks; #$P < 0.01$ vs. *Ncx1*$^{+/+}$ islets at 12 weeks. Cell viability was measured in isolated islet cells (*E*) and in intact islets (*F, G, H*) using Ho342 and PI staining in the absence or after 72-h exposure to thapsigargin (Thaps) or cyclopiazonic acid (CPA) (*E* and *G*), cytokines (Cyt; *F*), and after 6-h exposure to hypoxia (*H*). Mean ± SEM values are shown from four individual experiments. *F:* *$P < 0.05$ vs. control in the absence of cytokines. *G:* **$P < 0.01$ vs. respective *Ncx1* islets in the absence of Thaps. *H*: *$P < 0.05$ vs. *Ncx1*$^{+/+}$ islets.

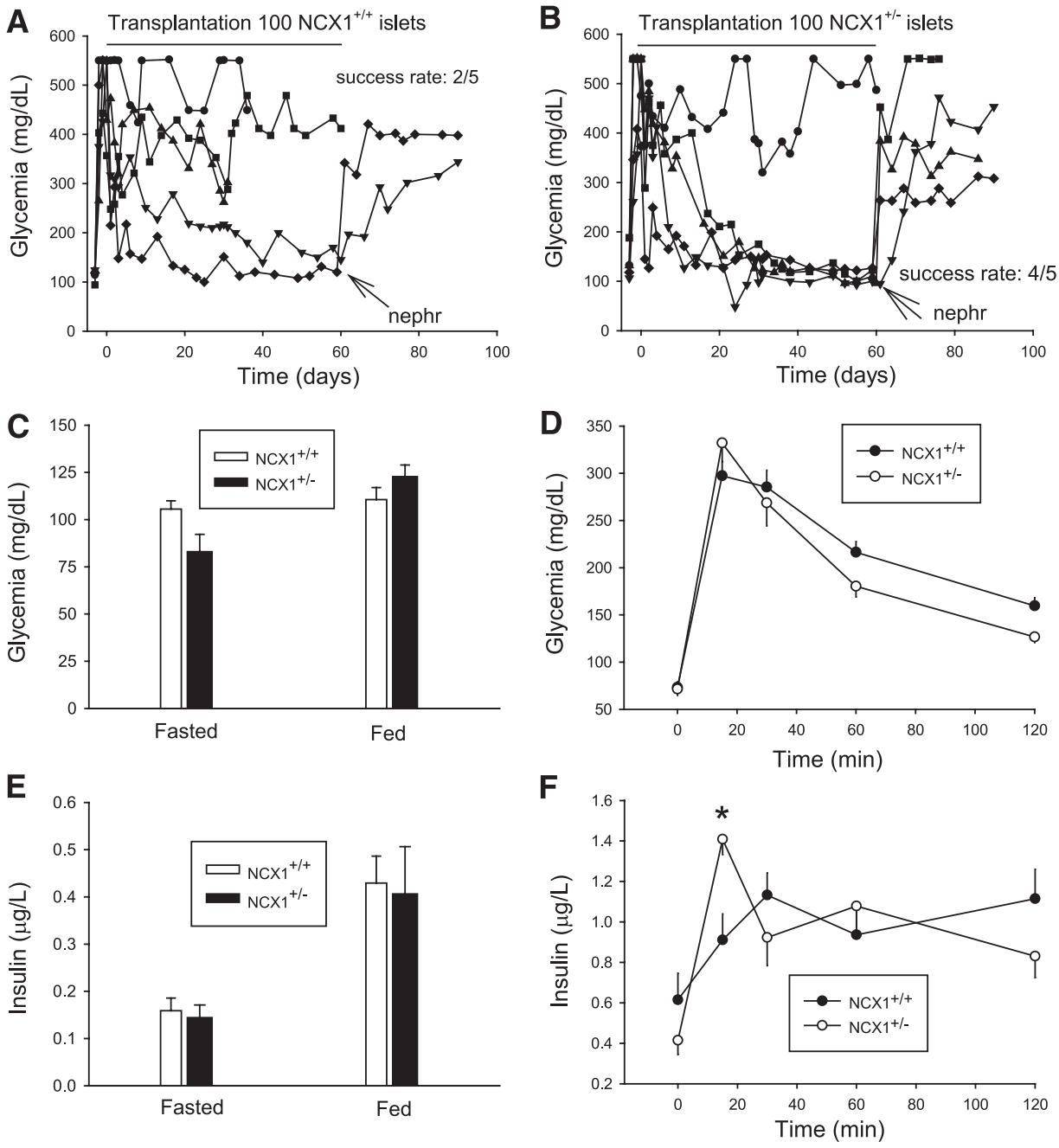

FIG. 6. Effect of *Ncx1* heterozygous inactivation on islets transplantation and glucose metabolism is shown in vivo. Effect of transplanting grafts of 100 islets from *Ncx1*$^{+/+}$ (*A*) or *Ncx1*$^{+/-}$ (*B*) mice is shown on nonfasting blood glucose levels. The success rate of diabetes cure (blood glucose level <220 mg/dL) was 2/5 for *Ncx1*$^{+/+}$ and 4/5 for *Ncx1*$^{+/-}$ islets. Nephr, nephrectomy. *C* and *E*: Glycemia and insulin levels measured in the fasting and the fed state of *Ncx1*$^{+/+}$ and *Ncx1*$^{+/-}$ mice (n = 5 in each case). *D* and *F*: Glycemia and insulin levels are shown during an intraperitoneal glucose tolerance test in *Ncx1*$^{+/+}$ and *Ncx1*$^{+/-}$ mice (n = 8 in each case). *P < 0.05. Data are shown as the means ± SEM.

ER Ca^{2+} stores. In a previous study we showed that NCX1 overexpression increased β-cell apoptosis and decreased β-cell proliferation by depleting ER Ca^{2+} stores (11). Therefore, we wondered whether the opposite changes seen in the current study in *Ncx1*$^{+/-}$ mice were not due to an increase in ER Ca^{2+} stores. To test this hypothesis, the effect of the SERCA inhibitor thapsigargin on $[Ca^{2+}]_i$ in pancreatic islets was examined (Supplementary Fig. 8). In *Ncx1*$^{+/+}$ islets, thapsigargin induced an important but transient increase in $[Ca^{2+}]_i$, a phenomenon that was increased by about 60% in *Ncx1*$^{+/-}$ islets ($P < 0.05$), indicating that ER Ca^{2+} stores were increased in *Ncx1*$^{+/-}$ compared with *Ncx1*$^{+/+}$ islets.

DISCUSSION

We generated a mouse strain with heterozygous inactivation of the gene coding for NCX1, the isoform of the Na/Ca exchanger that is expressed in the pancreatic β-cell (33). RT-PCR studies confirmed heterozygous inactivation of the exchanger in *Ncx1*$^{+/-}$ mice and the reduction of its expression in β-cells. The latter reduction led to a decrease in NCX1 activity as assessed at the physiologic

level, with inhibition of both modes of the exchanger (forward and reverse). The reduction in Na/Ca exchange activity in *Ncx1*$^{+/-}$ β-cells had multiple consequences:

First, as expected from cells from which Ca^{2+} extrusion is reduced, the rise in $[Ca^{2+}]_i$ induced by membrane depolarization and the uptake of ^{45}Ca induced by glucose were increased.

Second, the $[Ca^{2+}]_i$ oscillations induced by the sugar were disrupted. This was not unexpected, because the exchanger generates an inward current when working in its forward mode that contributes to the duration of the bursts of electrical activity (34) that underlie $[Ca^{2+}]_i$ oscillations (35,36). Hence, the reduction of the NCX1 inward current in *Ncx1*$^{+/-}$ cells led to the shortening and disorganization of the oscillations. However, in view of the decreased rate of ATP generation at high glucose in *Ncx1*$^{+/-}$ compared with *Ncx1*$^{+/+}$ islets, the disruption of the Ca^{2+} oscillations could also be due to an attenuation of the metabolic oscillations that underlie the slow electrical and Ca^{2+} oscillations via a relief of phosphofructokinase inhibition by ATP (37).

Third, glucose-induced insulin release was markedly increased. Both phases of insulin release were enhanced, which could also be related to the reduction in Ca^{2+} extrusion with subsequent increase in cellular Ca^{2+} content as objectified at the ER level. In view of this major increase in insulin release, we next examined insulin content, islet morphology, and glucose metabolism.

Insulin content was doubled in *Ncx1*$^{+/-}$ compared with *Ncx1*$^{+/+}$ β-cells, but no change in morphology was found between the cell types except for an increase in proinsulin staining in *Ncx1*$^{+/-}$ β-cells, a finding compatible with the increase in insulin content. In *Ncx1*$^{+/-}$ β-cells, there was a tendency toward an increase in glucose utilization at low glucose concentration and a significant decrease in glucose oxidation at high glucose concentration, making it unlikely that the observed increase in glucose-induced insulin release in these islets is explained by an augmented mitochondrial glucose metabolism. The increase in the insulin secretory rate may result instead from increased insulin production and cellular Ca^{2+} content.

We next looked at β-cell mass, size, proliferation, and death. At 12 weeks (adult mice), β-cell mass had increased 100% in *Ncx1*$^{+/-}$ compared with *Ncx1*$^{+/+}$ mice, a phenomenon that was not due to an increase in β-cell size but rather to an increase in β-cell proliferation, the rate of which was five-times higher in *Ncx1*$^{+/-}$ mice than in *Ncx1*$^{+/+}$ mice. The view that a decrease in β-cell death could also contribute to this observation was examined, but the results obtained were negative except in the case of hypoxia. Indeed, although measurement by the TUNEL method showed no difference in the rate of apoptosis under basal conditions and no difference in viability between single cells or islets of *Ncx1*$^{+/+}$ and *Ncx1*$^{+/-}$ mice under basal and stimulated conditions, *Ncx1*$^{+/-}$ islets showed a 37% protection against hypoxia compared with *Ncx1*$^{+/+}$ islets.

The increase in β-cell function, growth, and resistance to the physiologic stress of *Ncx1*$^{+/-}$ islets was confirmed in transplantation studies, the *Ncx1*$^{+/-}$ islets being at least twice as efficient in curing diabetes than the *Ncx1*$^{+/+}$ islets. In this respect, it is important to know that islets transplantation represents a valuable approach in the treatment of diabetes. However, its applicability is limited by the need to transplant a high number of islets from two or more donors. In clinical islet transplantation, it has been estimated that up to 70% of the transplanted β-cell mass is destroyed in the early post-transplant period due to non–immune-mediated physiologic stress, namely prolonged hypoxia during the revascularization process (38).

The increase in insulin content, β-cell proliferation, and mass seen in *Ncx1*$^{+/-}$ islets could result from the activation by raised cellular Ca^{2+} of the calcineurin/nuclear factor of activated T-cell (NFAT) signaling pathway. Calcineurin is a calmodulin-dependent serine/threonine phosphatase that dephosphorylates the cytoplasmic subunits of NFAT (NFATc) upon activation by Ca^{2+}. Dephosphorylation of NFATc allows its rapid translocation to the nucleus, with subsequent activation of insulin transcription and promotion of β-cell proliferation by increasing the expression of cell cycle promoters such as cyclin D1, cyclin D2, and cyclin-dependent kinase 4 (CDK4) (39). β-Cell–specific calcineurin inactivation in knockout mice impaired insulin transcription and cyclins expression, leading to markedly decreased β-cell proliferation and mass and to diabetes onset (40). Interestingly, calcineurin inactivation did not increase β-cell apoptosis (39), a finding compatible with the absence of a decrease in β-cell apoptosis observed in this study.

Last, except for a higher initial peak of insulin release during the glucose tolerance test, no difference was found in in vivo glucose metabolism or in insulin resistance between both mice.

In conclusion, heterozygous inactivation of a single gene (*Ncx1*) leads to an increase in insulin release, β-cell proliferation and mass, and to an increase in resistance to β-cell death, namely, to various changes in β-cell function that are opposite to the major abnormalities seen in type 2 diabetes. Moreover, it increased the success rate of islet transplantation in diabetic animals. Downregulation of the β-cell Na/Ca exchanger is thus a unique model providing a novel concept for the prevention and treatment of type 2 diabetes and to improve the applicability of islet transplantation.

ADDENDUM

During the process of submitting the present work for publication, another study showed that KB-R7943, an NCX1 inhibitor, enhanced glucose-induced insulin release, a finding confirming part of our results (41).

ACKNOWLEDGMENTS

This work was supported by grants from the Belgian Fund for Scientific Research (FRSM 3.4593.04, 3.4527.08), the European Foundation for the Study of Diabetes/Novo Nordisk Programme in Diabetes Research (2005/6), the Juvenile Diabetes Research Foundation International (1-2008-536), the Communauté Française de Belgique–Actions de Recherche Concertées (ARC), the European Union (Integrated Project Naimit [FP7] of the European Community), and the Belgium Program on Interuniversity Poles of Attraction initiated by the Belgium State (IUAP P6/40). CIBERDEM is an initiative of Instituto de Salud Carlos III (Spain). A.K.C. is a Research Associate, and J.-M.V. is a Research Director of the Fonds National de la Recherche Scientifique. F.A. was supported by a fellowship from the "Crédit de Relations Internationales de l'Université Libre de Bruxelles". G.J. was supported by a grant from the Fundació Privada Institut d'Investigació Biomedica de Bellvitge. No other potential conflicts of interest relevant to this article were reported.

E.N., S.So., S.B., N.P., and E.D. researched data and contributed to discussion. F.A., J.-M.V., and A.S. researched data, contributed to discussion, and reviewed and edited the manuscript. M.M., M.D., J.M., and G.J. researched data and contributed to discussion. E.M., J.R., A.K.C., and D.L.E. researched data, contributed to discussion, and reviewed and edited the manuscript. S.Sc. researched data and contributed to discussion. A.H. researched data, contributed to discussion, and wrote the manuscript.

The authors thank A. Van Praet, A. Iabkriman, and M.P. Berghmans (Laboratory of Pharmacology, Université Libre de Bruxelles) for excellent technical support.

REFERENCES

1. King H, Aubert RE, Herman WH. Global burden of diabetes, 1995-2025: prevalence, numerical estimates, and projections. Diabetes Care 1998;21:1414–1431
2. Yang W, Lu J, Weng J, et al.; China National Diabetes and Metabolic Disorders Study Group. Prevalence of diabetes among men and women in China. N Engl J Med 2010;362:1090–1101
3. Utzschneider KM, Kahn SE. β-cell dysfunction in type 2 diabetes. In *International Textbook of Diabetes Mellitus*. DeFronzo RA, Ferrannini E, Keen H, Zimmet P, Eds. Hoboken, NJ, John Wiley & Sons, Ltd, 2003, p. 375–388
4. Porte D Jr. Banting lecture 1990. Beta-cells in type II diabetes mellitus. Diabetes 1991;40:166–180
5. Kahn SE, Zraika S, Utzschneider KM, Hull RL. The beta cell lesion in type 2 diabetes: there has to be a primary functional abnormality. Diabetologia 2009;52:1003–1012
6. MacLean N, Ogilvie RF. Quantitative estimation of the pancreatic islet tissue in diabetic subjects. Diabetes 1955;4:367–376
7. Rahier J, Guiot Y, Goebbels RM, Sempoux C, Henquin JC. Pancreatic beta-cell mass in European subjects with type 2 diabetes. Diabetes Obes Metab 2008;10(Suppl. 4):32–42
8. Cnop M, Welsh N, Jonas JC, Jörns A, Lenzen S, Eizirik DL. Mechanisms of pancreatic beta-cell death in type 1 and type 2 diabetes: many differences, few similarities. Diabetes 2005;54(Suppl. 2):S97–S107
9. Blaustein MP, Lederer WJ. Sodium/calcium exchange: its physiological implications. Physiol Rev 1999;79:763–854
10. Philipson KD, Nicoll DA, Ottolia M, et al. The Na^+/Ca^{2+} exchange molecule: an overview. Ann N Y Acad Sci 2002;976:1–10
11. Diaz-Horta O, Kamagate A, Herchuelz A, Van Eylen F. Na/Ca exchanger overexpression induces endoplasmic reticulum-related apoptosis and caspase-12 activation in insulin-releasing BRIN-BD11 cells. Diabetes 2002;51:1815–1824
12. Sokolow S, Manto M, Gailly P, et al. Impaired neuromuscular transmission and skeletal muscle fiber necrosis in mice lacking Na/Ca exchanger 3. J Clin Invest 2004;113:265–273
13. Van Eylen F, Lebeau C, Albuquerque-Silva J, Herchuelz A. Contribution of Na/Ca exchange to Ca^{2+} outflow and entry in the rat pancreatic beta-cell: studies with antisense oligonucleotides. Diabetes 1998;47:1873–1880
14. Plasman PO, Lebrun P, Herchuelz A. Characterization of the process of sodium-calcium exchange in pancreatic islet cells. Am J Physiol 1990;259:E844–E850
15. Herchuelz A, Malaisse WJ. Regulation of calcium fluxes in pancreatic islets: dissociation between calcium and insulin release. J Physiol 1978;283:409–424
16. Malaisse WJ, Sener A. Hexose metabolism in pancreatic islets. Feedback control of D-glucose oxidation by functional events. Biochim Biophys Acta 1988;971:246–254
17. Hutton JC, Sener A, Malaisse WJ. The metabolism of 4-methyl-2-oxopentanoate in rat pancreatic islets. Biochem J 1979;184:291–301
18. Sempoux C, Guiot Y, Dahan K, et al. The focal form of persistent hyperinsulinemic hypoglycemia of infancy: morphological and molecular studies show structural and functional differences with insulinoma. Diabetes 2003;52:784–794
19. Jacoby M, Cox JJ, Gayral S, et al. INPP5E mutations cause primary cilium signaling defects, ciliary instability and ciliopathies in human and mouse. Nat Genet 2009;41:1027–1031
20. Mast J, Nanbru C, van den Berg T, Meulemans G. Ultrastructural changes of the tracheal epithelium after vaccination of day-old chickens with the La Sota strain of Newcastle disease virus. Vet Pathol 2005;42:559–565
21. Téllez N, Montolio M, Biarnés M, Castaño E, Soler J, Montanya E. Adenoviral overexpression of interleukin-1 receptor antagonist protein increases beta-cell replication in rat pancreatic islets. Gene Ther 2005;12:120–128
22. Teta M, Long SY, Wartschow LM, Rankin MM, Kushner JA. Very slow turnover of β-cells in aged adult mice. Diabetes 2005;54:2557–2567
23. Cardozo AK, Ortis F, Storling J, et al. Cytokines downregulate the sarcoendoplasmic reticulum pump Ca^{2+} ATPase 2b and deplete endoplasmic reticulum Ca^{2+}, leading to induction of endoplasmic reticulum stress in pancreatic β-cells. Diabetes 2005;54:452–461
24. Biarnés M, Montolio M, Nacher V, Raurell M, Soler J, Montanya E. Beta-cell death and mass in syngeneically transplanted islets exposed to short- and long-term hyperglycemia. Diabetes 2002;51:66–72
25. Emamaullee JA, Rajotte RV, Liston P, et al. XIAP overexpression in human islets prevents early posttransplant apoptosis and reduces the islet mass needed to treat diabetes. Diabetes 2005;54:2541–2548
26. Brüning JC, Winnay J, Bonner-Weir S, Taylor SI, Accili D, Kahn CR. Development of a novel polygenic model of NIDDM in mice heterozygous for IR and IRS-1 null alleles. Cell 1997;88:561–572
27. Lenzen S. The mechanisms of alloxan- and streptozotocin-induced diabetes. Diabetologia 2008;51:216–226
28. Koushik SV, Wang J, Rogers R, et al. Targeted inactivation of the sodium-calcium exchanger (Ncx1) results in the lack of a heartbeat and abnormal myofibrillar organization. FASEB J 2001;15:1209–1211
29. Gilon P, Shepherd RM, Henquin JC. Oscillations of secretion driven by oscillations of cytoplasmic Ca^{2+} as evidences in single pancreatic islets. J Biol Chem 1993;268:22265–22268
30. Bergsten P, Grapengiesser E, Gylfe E, Tengholm A, Hellman B. Synchronous oscillations of cytoplasmic Ca^{2+} and insulin release in glucose-stimulated pancreatic islets. J Biol Chem 1994;269:8749–8753
31. Malaisse WJ, Sener A, Herchuelz A, Hutton JC. Insulin release: the fuel hypothesis. Metabolism 1979;28:373–386
32. Malaisse-Lagae F, Malaisse WJ. The stimulus-secretion coupling of glucose-induced insulin release. 3. Uptake of ^{45}calcium by isolated islets of Langerhans. Endocrinology 1971;88:72–80
33. Van Eylen F, Svoboda M, Herchuelz A. Identification, expression pattern and potential activity of Na/Ca exchanger isoforms in rat pancreatic B-cells. Cell Calcium 1997;21:185–193
34. Gall D, Gromada J, Susa I, Rorsman P, Herchuelz A, Bokvist K. Significance of Na/Ca exchange for Ca^{2+} buffering and electrical activity in mouse pancreatic β-cells. Biophys J 1999;76:2018–2028
35. Perez-Armendariz E, Atwater I. Glucose-evoked changes in $[K^+]$ and $[Ca^{2+}]$ in the intercellular spaces of the mouse islet of Langerhans. Adv Exp Med Biol 1986;211:31–51
36. Henquin JC, Jonas JC, Gilon P. Functional significance of Ca^{2+} oscillations in pancreatic beta cells. Diabetes Metab 1998;24:30–36
37. Lenzen S, Lerch M, Peckmann T, Tiedge M. Differential regulation of $[Ca^{2+}]_i$ oscillations in mouse pancreatic islets by glucose, α-ketoisocaproic acid, glyceraldehyde and glycolytic intermediates. Biochim Biophys Acta 2000;1523:65–72
38. Emamaullee JA, Shapiro AM. Perspectives in diabetes. Interventional strategies to prevent β-cell apoptosis in islet transplantation. Diabetes 2006;55:1907–1914
39. Heit JJ. Calcineurin/NFAT signaling in the beta-cell: From diabetes to new therapeutics. Bioessays 2007;29:1011–1021
40. Heit JJ, Apelqvist AA, Gu X, et al. Calcineurin/NFAT signalling regulates pancreatic beta-cell growth and function. Nature 2006;443:345–349
41. Hamming KSC, Soliman D, Webster NJ, et al. Inhibition of β-cell sodium-calcium exchange enhances glucose-dependent elevations in cytoplasmic calcium and insulin secretion. Diabetes 2010;59:1686–1693